

BUCKLING OF SKEW PLATES WITH CONTINUITY OR ROTATIONAL EDGE RESTRAINT

P. Huyton and C. B. York

Division of Engineering, The University of Edinburgh
Crew Building, The King's Buildings, Edinburgh. EH9 3JN

Keywords: *Elastic buckling, elastic rotational restraint, finite element analysis, in-plane compression, skew plates, continuous plates, buckling modes*

Abstract

Buckling strength predictions are presented for a wide range of thin isotropic skew plates, subject to uniform uniaxial compression. The key studied parameters include the aspect ratio, skew angle and rotational restraint stiffness on the different edges of the plate. The buckling strengths are evaluated both for isolated plates and for plates which are continuous with other parts of the structure. The buckling predictions are presented in the form of dimensionless buckling curves, which permits a ready adoption into the "data sheets" commonly used in current design.

1 Introduction

In most buckling studies of skew plates, the adopted boundary conditions have been restricted to either clamped, simply supported, free or combinations of these. Although these boundary conditions are useful in providing upper- or lower-bound solutions to a more general problem, they lead to loss of economy in design because they do not permit the benefits of restraint and continuity to be included safely in the design process. In real structures there is continuity between adjacent panels and other structural elements, which offer both bending and torsional stiffness to the plate edges.

The well-known data sheets [6, 7] are widely used in hand calculation of buckling assessments, but their content is restricted to the sim-

pler buckling load, geometry and boundary condition cases, and the significant body of work which now exists dealing with the effects of rotational edge stiffness has not yet been adopted partly because it is incomplete. This paper reviews, collates and extends this body of work and presents a comprehensive, compact series of design curves that illustrate the effect of introducing symmetrical combinations of elastic rotational restraints on the edges of isolated skew plates. The paper also presents a unique comparison of previous studies for plates that are continuous over skew bays. The new buckling predictions of this paper illustrate the complex nature of the mode changes, which often lead to local strength optima in skew plate structures.

2 Background

Rotational restraint along the edges of a plate arises from two physical characteristics: the torsional stiffness of a supporting spar, rib or stiffener and the restraint imposed by continuity over a support, which itself may possess no torsional stiffness. These two stiffnesses are additive and provide a rotational restraint on the edges of an isolated plate which can be exploited to determine increased buckling strengths when the plate forms an integral part of a larger continuous plate structure.

Much of the earliest work on the buckling of skew plates is described in the monographs of Timoshenko [18] and Morley [17]. Both upper-

bound [9] and lower-bound [10] solutions have been obtained for clamped skew plates subject to uniform compression using the Lagrangian multiplier method. Upper-bound solutions have also been found using the Raleigh-Ritz method with Iguchi deflection functions [19]. Solutions for simply supported skew plates have since been obtained by several other methods, including the Galerkin method [5]; the energy method with Fourier series to describe the deflected shape [12] and the finite element method [8, 11]. Solutions have also been developed for skew plates under uniform shear loading with similar boundary conditions [20, 25, 3, 4, 15, 21] as well as some specific cases for mixed boundary conditions in compression loaded plates involving free, simply supported and clamped conditions [16].

There are very few buckling solutions for skew plates with rotationally restrained edges or for plates continuous over skew bays: the B-spline method was used [13] to obtain critical compression loads for skew plates with rotational restraints along the loaded skew edges; the energy method was adopted [2] to analyse a continuous plate over skew bays in both transverse and longitudinal directions subject to uni-axial and bi-axial compression loading and; more recently, a modified procedure [24] based on the stiffness matrix method incorporating Lagrangian multipliers was used to investigate [22] the differences in buckling strength between skew plates with continuity in the longitudinal direction and continuity in both longitudinal and transverse directions when subject to compression or shear loading.

3 Theoretical Approach

Eigenvalue extraction is performed using a commercial finite element program [1] for the simply supported skew plates with added rotational edge restraints. A more limited number of buckling predictions are obtained by a stiffness matrix method [24] incorporating Lagrangian multipliers. This method is based on the assumption that the plate is of infinite length (and width), accounting for plates continuous over skew bays.

Agreement between the two methods is expected only for the clamped cases, whereby the continuous plate degenerates into a series of clamped plates joined end to end.

4 Computational Modelling

Thin isotropic plates were considered under uniform in-plane compressive stress applied to the skew-transverse edges.

Three different skew angles 15° , 30° & 45° are considered, each with aspect-ratios in the range $0.5 \leq a/b \leq 2.5$. The material properties were chosen as Young's modulus $E = 72.4 \text{ kN/mm}^2$ ($10.5 \times 10^6 \text{ psi}$) and Poisson's ratio, $\nu = 0.3$. These choices allow direct comparison with existing buckling predictions for continuous plates [22].

For the finite element analysis, an S8R5 element was adopted to obtain a thin-plate solution. Unlike rectangular plates ($\alpha = 0^\circ$), high stresses are known to develop at the obtuse corners of skew plates [14] and a high mesh density was therefore adopted to model these adequately. Following a careful convergence study on a plate with $\alpha = 45^\circ$, a uniform mesh of 30×30 elements for the aspect-ratio $a/b = 1$ was found to give predictions within 3% of the converged result. The same mesh density was retained for other aspect-ratios (*i.e.* a 30×75 mesh was chosen for $a/b = 2.5$).

The buckling predictions are expressed in terms of the non-dimensional buckling coefficient:

$$k = \frac{\sigma b^2 t}{\pi^2 D} \quad (1)$$

where:

- σ is the critical buckling stress
- b is the skew-transverse side length of the plate,
- t is the thickness of the plate and
- D is the flexural rigidity of the plate.

Rotational restraint was added to the plate edges using a number of single degree of freedom spring elements, restricting rotation normal to the longitudinal and skew-transverse edges in order to approximate the physical restraint in a continuous plate. The stiffness of the rotational edge restraint can be characterised in non-dimensional form using the coefficient,

$$\kappa = \frac{\beta b}{D} \quad (2)$$

where β is the elastic stiffness against rotation per unit length of plate edge.

5 Results

The plate geometry is shown above each design curve in Figures 1 and 2, where side lengths a and b , principal axes, boundary conditions and applied loading are defined. Boundary conditions are described throughout the paper using the notation ‘Case $x - y$ ’, where the integers x and y identify the boundary conditions along the longitudinal (x) and skew-transverse (y') edges, respectively, as:

1. simply supported;
2. elastically restrained against rotation;
3. continuous over otherwise simple supports and;
4. rotationally clamped.

Thus Case 1-1 refers to a simply supported plate; Case 1-2 includes elastic restraints against rotation along the loaded, skew-transverse (y') edges of the plate; Case 1-3 refers to a plate which has continuity in the x -direction over skew-transverse supports with simply supported longitudinal, unloaded edges and; Case 1-4 has loaded edges rotationally clamped ($\kappa = \infty$).

The buckling design curves of Figures 1 and 2 show the variation of dimensionless critical stress with plate aspect ratio. They illustrate the effect of increasing the stiffness of the elastic restraint against rotation along symmetrical

edges of a plate. This stiffness is expressed in non-dimensional terms with values of $\kappa = 0.4, 1, 2, 4, 10, 20$ & ∞ . The same stiffness values are used throughout the paper, except where curves have been omitted for clarity.

Each curve was derived from 21 buckling calculations, representing the side-ratios $a/b = 0.5, 0.6, 0.7, \dots, 2.5$, through which a spline curve was then generated. Wherever a buckling mode transition caused a cusp, further critical buckling stresses were obtained with additional buckling calculations. Each figure contains three adjacent sets of curves for ease of comparison, representing the skew angles $\alpha = 15^\circ, 30^\circ$ and 45° .

The changes in buckling mode associated with the curves of Figures 1 and 2 are shown in Figures 3 and 4. These indicate that quite radical mode changes occur as the aspect ratio is changed, so that simple assumptions about the form or direction of nodal lines may be valid at one aspect ratio and invalid at another.

To provide a measure of the potential strength gains from rotational edge restraint, the ratio of the buckling strengths of a simply supported plate to that of the corresponding clamped plate is shown in Figure 5, which provides a datum for the potential strength gains achieved by continuity illustrated in Figure 6. The following section provides a detailed discussion of these results.

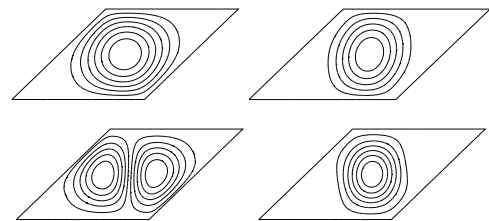


Fig. 3 Buckling modes for a 45° skew plate with aspect-ratio $a/b = 1$ and: all edges simply supported (top-left); skew-transverse edges clamped (top-right); longitudinal edges clamped (bottom-left) and; all edges clamped (bottom-right).

6 Discussion of Results

The buckling curves of Figures 1 and 2 are in the classic form of garland curves corresponding to

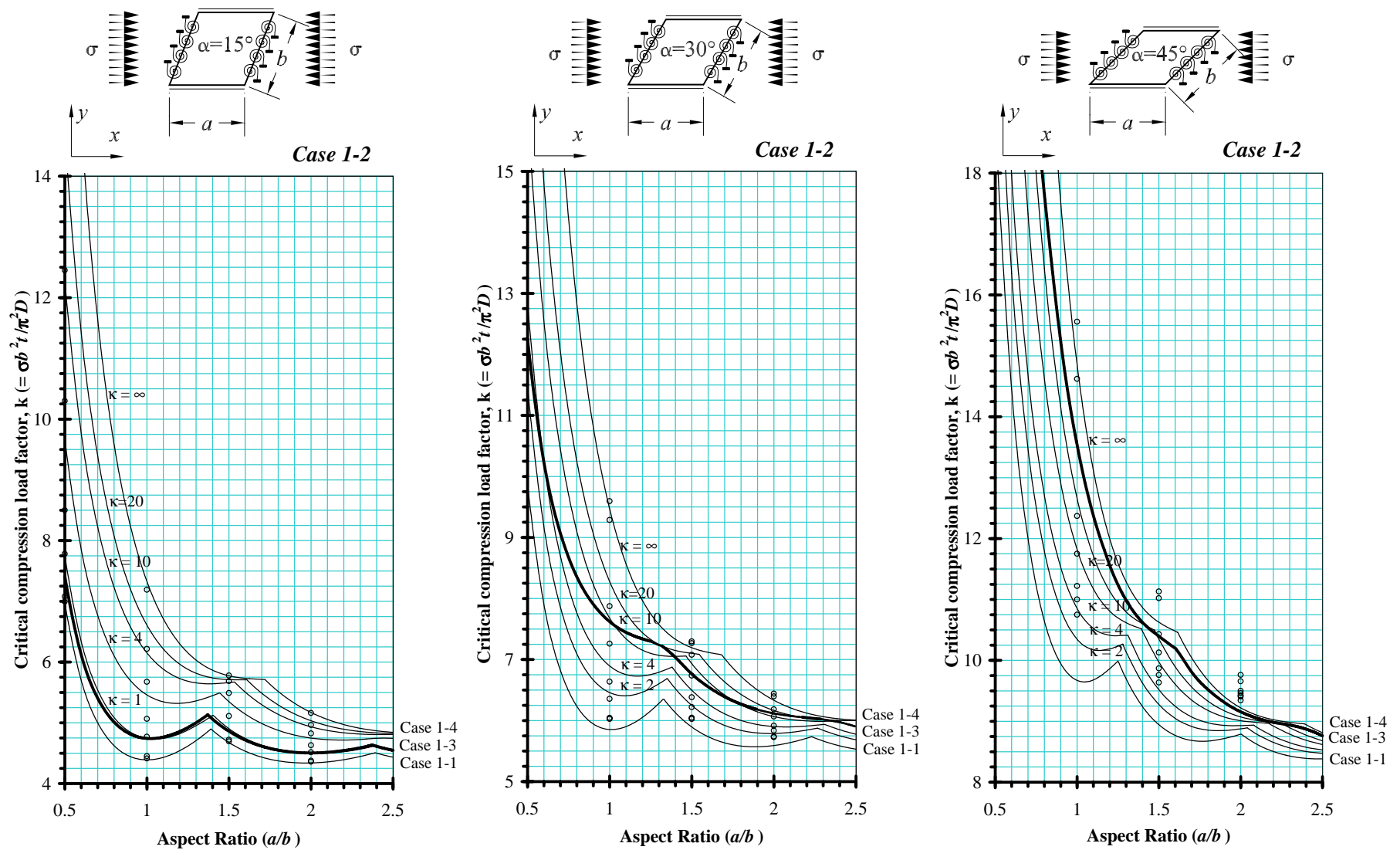


Fig. 1 Case 1-2 design curves for $\alpha = 15^\circ, 30^\circ$ & 45° with skew-transverse edges elastically restrained against rotation and longitudinal edges simply supported.

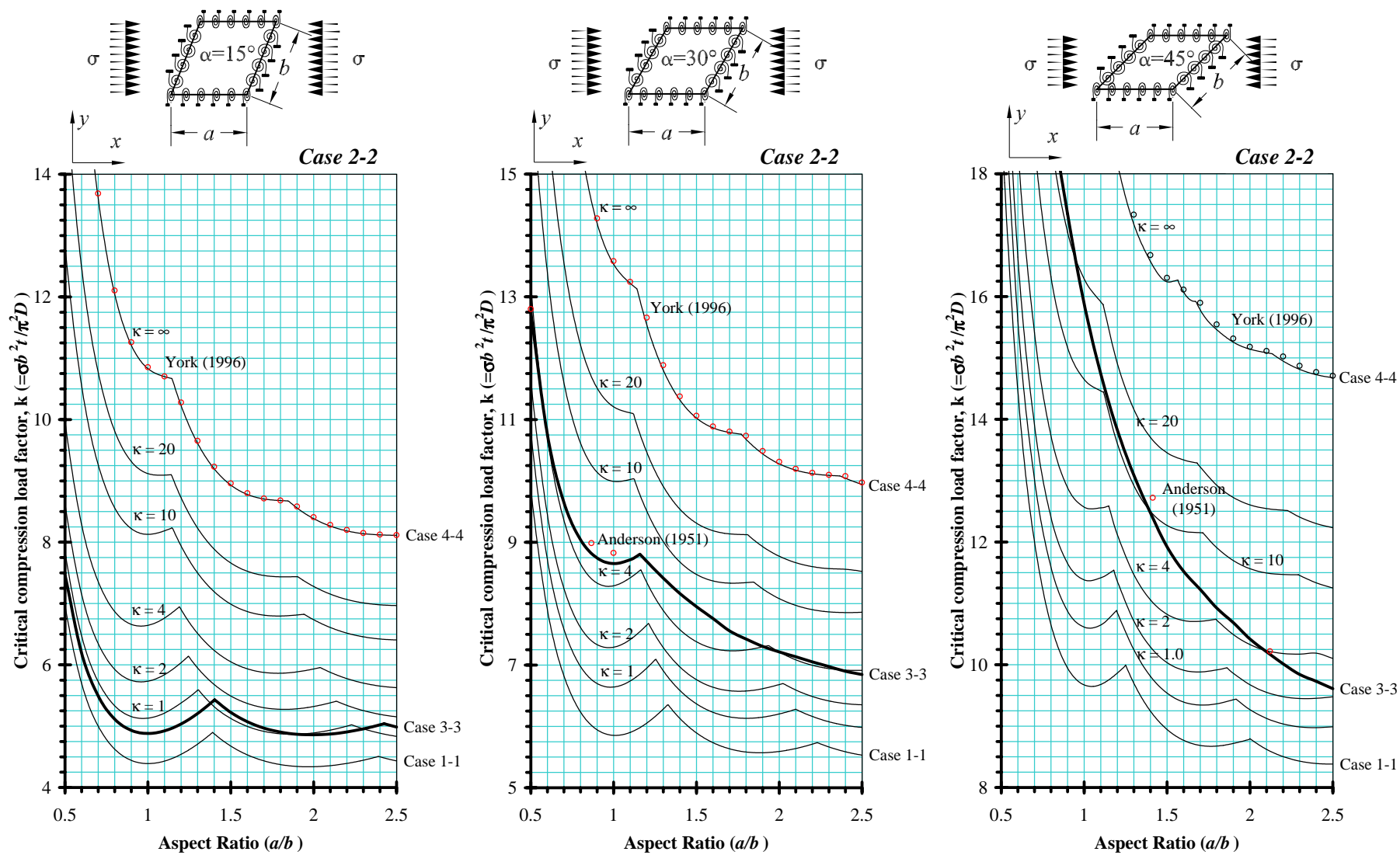


Fig. 2 Case 2-2 design curves for $\alpha = 15^\circ, 30^\circ$ & 45° with all edges elastically restrained against rotation.

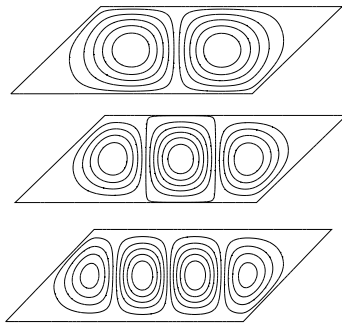


Fig. 4 Buckling modes for the 45° skew plate of constant aspect-ratio ($a/b = 1.9$) with all edges: simply supported (top), restraint against rotation with $\kappa = 10$ (middle) and clamped ($\kappa = \infty$).

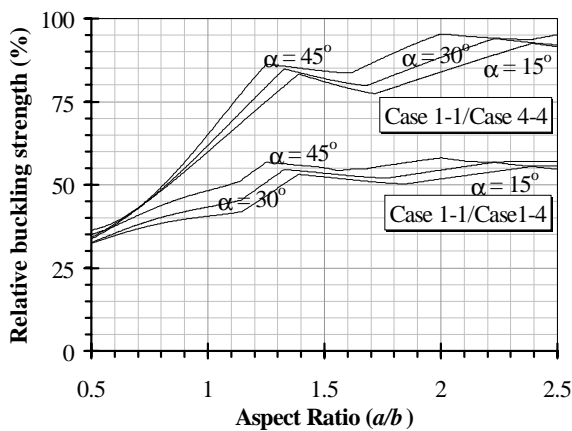


Fig. 5 Relative buckling strength of a simply supported plate when compared with plates having clamped boundary conditions along loaded edges (Case 1-1/Case 1-4) and all edges (Case 1-1/Case 4-4).

different modes with cusps at the aspect ratios of coincident modes. The location of the cusp between one mode and another can be seen to depend strongly on the skew angle and less strongly on the stiffness of the rotational restraint on the plate edges. The dimensionless buckling coefficient k also increases substantially as the skew angle increases, though the asymptotic value at large aspect ratios is naturally independent of the skew.

By comparing the figures, it can be seen that the boundary conditions along the unloaded longitudinal edges have a powerful influence on the buckling strengths for plates of this kind.

The wide spread of the buckling curves in Figure 2 indicates the sensitivity to changes in boundary conditions along the unloaded edges, whereas Figure 1 shows little increase in buckling strength with changes in rotational stiffness along the skew-transverse edges, particularly for high aspect-ratio.

The appearance of this effect is influenced by the fact that the aspect ratio has been defined (to permit direct comparisons with earlier studies) in terms of the plate side lengths a and b , so that an increase in skew angle (α) corresponds to a reduction in the distance between parallel sides. An increase in skew angle therefore leads to an increase in aspect ratio (a/b'), where $b' (= b \cdot \cos \alpha)$ is the plate width measured normal to the x -axis.

The buckling strengths of a plate continuous over skew-transverse edges [22] and an isolated skew plate are compared in Fig. 1. The gain in buckling strength provided by continuity increases with skew angle. Further comparisons are also shown in Fig. 1 for skew plates with their loaded edges elastically restrained against rotation [13]. Whilst there is a close similarity between the effects of rotational restraint at low aspect ratios, this match is progressively lost with increasing skew angle.

The buckling strengths of skew plates with continuity over all edges [22] are shown as bold lines in Figure 2. Here an even greater strength advantage can be seen over the isolated plate counter-part. A close correlation can be seen here between the rotationally clamped ($\kappa = \infty$) predictions and those for continuous plates [22] which degenerate into an array of clamped skew plates in this case.

The buckling mode of a compression loaded skew plate may be compared with that of a shear loaded rectangular plate, where nodal lines of the buckling mode are no longer consistent with transverse edges [17]. For the continuous plate, a mode interaction develops between the adjacent plates with a period that may repeat over several bay lengths, giving rise to the marked differences between the continuous and isolated plate cases in both buckling strength and mode. By contrast, a rectangular compression loaded plate ($\alpha = 0^\circ$)

displays no comparable strength gain, because the buckling mode is symmetric and repeats with an equal and opposite deflection pattern in adjacent bays [23]. Despite Anderson's [2] simplifying assumptions about the buckle pattern in his energy formulation for continuous skew plates, his results agree well with predictions from the more rigorous analysis [24] illustrated in Figure 2.

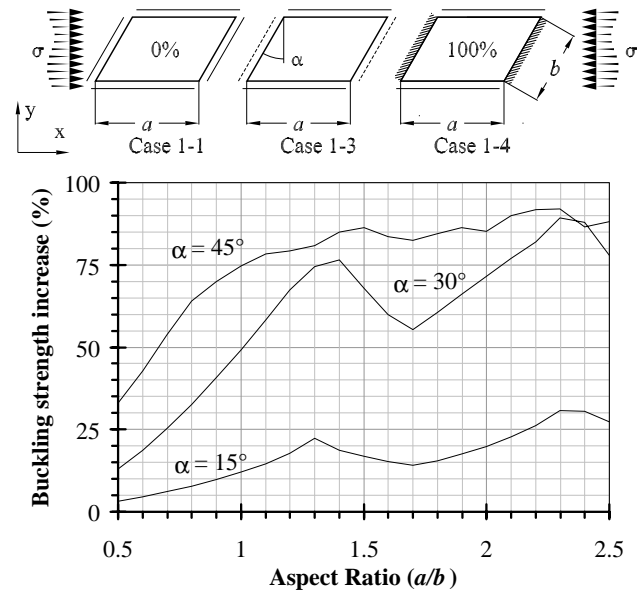
In the buckling strength curves of Figs 1 and 2, the cusps that indicate a change in the buckling mode can be seen to form sweeping patterns across all the figures. These patterns arise as a direct consequence of increasing rotational edge restraint, which effectively foreshortens the plate length a when restraint is applied to the loaded, skew-transverse edges. Rotational edge restraint thus causes an increase in the number of mode changes over a given range of aspect-ratios. The opposite is true when longitudinal edges are restrained, causing a decrease in the number of mode changes.

The buckling modes which occur for different combinations of edge restraint are shown in Figure 3. A simply supported plate is shown in the top left of the figure, which may be compared, moving clockwise around the figure, with modes arising from the clamping of the skew-transverse edges, all edges and the longitudinal edges respectively. In each case, the half-wavelength of the buckled mode is foreshortened normal to the restrained edges of the plate, giving rise to a change in mode from one to two half-wavelengths when longitudinal edges are clamped.

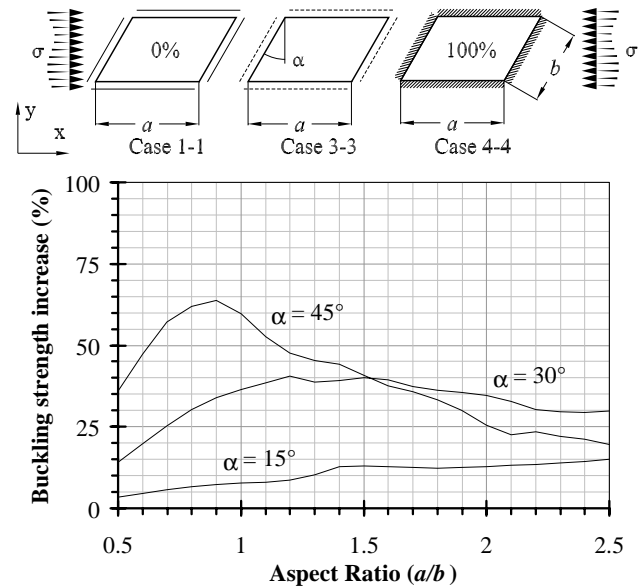
The buckling modes of three plates with the same aspect ratio ($a/b = 1.9$) are shown in Figure 4. The mode changes containing two, three and four half-waves respectively, are a result of increasing the magnitude of the rotational restraint ($\kappa = 0, 10 \text{ \& } \infty$) to all four edges of the plate.

The cusps in Figures 1 and 2 between different buckling modes offer a useful opportunity for optimisation of the plate if the aspect ratio is carefully chosen. The current data sheets offer no comparable information for skew plate design. The new curves may therefore assist the designer

to select the plate aspect ratio to achieve an optimum strength when either continuity or elastic restraint against rotation can be relied upon in the structure.



(a) Continuity over skew-transverse edges



(b) Continuity over all four edges

Fig. 6 Relative increase in buckling strength arising from skew plates: (a) skew-transverse edges (Case 1-3) and; (b) all four edges (Case 3-3).

Figures 1 and 2 also show that the buckling strength of a continuous plate is comparable with that of an isolated plate whose edges are elastically restrained against rotation in a limited number of cases. This correlation is however severely affected by the more complex mode interactions arising in the continuous plate.

Note that in practice, rotational stiffness exists in combination with the effects of continuity.

The rotational stiffness is provided by a supporting spar or stiffener, adjacent plate or other structure, whose torsional characteristics may be affected by stress states in adjacent parts of the structure. The discrete spring elements which have been used in the current analysis to approximate a medium providing elastic restraint against rotation may therefore be a rather simplified model to account for the full effects of continuity.

The potential strength gains from edge rotational restraint ($\kappa = \infty$) applied along either the skew-transverse edges or all edges of the plate are shown in Figure 5. At low aspect ratio these gains are relatively small (35%) but above aspect ratio $a/b = 1.2$ a high strength plateau is reached, which corresponds to an increase of over 50% for plates with restraint applied to skew-transverse edges only, and above 75% for plates with all edges restrained. The relative proportion of these gains which are realised by continuity are shown in Figure 6 where three illustrations along the top of the figure help to illustrate the comparisons. The base reference case (0% = all edges simply supported) is common to all the comparisons, but the upper-bound reference cases (100%) differ according to the boundary conditions considered. The curves of Figure 6(a) show an increasing trend in relative buckling strength over the range of aspect ratios investigated; the occasional local reductions in the relative strength corresponding to asynchronous changes in buckling mode between the rotationally restrained and continuous plate, see Figure 1. The rate of increase in strength is more pronounced at higher skew angles due the relative increases in aspect ratio that were discussed earlier.

In contrast, Fig. 6(b) shows high initial

strength gains are lost with increasing aspect ratios through the addition of longitudinal edge restraint, giving continuity over all edges, as shown in the illustrations above the figure. In this case the longitudinal boundary conditions have a more dominant effect on the buckling strength as side length a is increased.

7 Conclusions

A compact set of design curves has been presented for the buckling assessment of isotropic skew plates under uniform, uni-axial compression load. The new curves illustrate the changes in buckling strength arising from the addition of symmetric combinations of elastic edge restraints against rotation for a wide range of aspect-ratios and skew angles. The new curves provide the designer with a greater insight into the buckling behaviour of skew plates and continuous plate structures. They allow more appropriate selection of plate aspect-ratio in order to achieve significant strength gains when continuity or elastic restraint against rotation exists in the structure and which would otherwise be missed if designs are based on the limited information currently available. The curves also provide new design information useful in predicting the increase in buckling strength provided by a continuous plate structure above that of an isolated plate counterpart, on which many current plate designs are based.

8 Acknowledgements

The Engineering and Physical Sciences Research Council is gratefully acknowledged in respect of the studentship award (Grant No. GR/L86661) which supported the first author.

References

- [1] *ABAQUS Users' manual, Version 5.8*. Hibbit, Karlsson and Sorensen Inc., Warrington, Cheshire, U.K., 1998.
- [2] Anderson R. Charts giving critical compressive stress of continuous flat sheet divided into

- parallelogram-shaped panels. Technical Report TN 2392, NACA, July 1951.
- [3] Ashton J. Stability of clamped skew plates under combined loads. *Journal of Applied Mechanics*, Vol. 36, No 1, pp 139–140, 1969.
- [4] Durvasula S. Buckling of clamped skew plates. *AIAA Journal*, Vol. 8, No 1, pp 178–181, 1970.
- [5] Durvasula S. Buckling of simply supported skew plates. *Proceedings of the ASCE, Journal of the Engineering Mechanics Division*, Vol. 97, No 3, pp 967–979, 1971.
- [6] ESDU 02.01.46. ESDU 02.01.46: Buckling stress coefficients for flat parallelogram plates under uniform compression (all edges fixed against rotation). Technical report, Engineering Sciences Data Unit, June 1957. Reprinted, February 1969.
- [7] ESDU 02.01.47. ESDU 02.01.47: Buckling stress coefficients for parallelogram shaped panels in continuous flat sheet under uniform compression. Technical report, Engineering Sciences Data Unit, 1957. Reprinted with Amendment A, April 1984.
- [8] Fried I and Schmitt K. Numerical results from the application of gradient iterative techniques to the finite element vibration and stability analysis of skew plates. *Aeronautical Journal*, Vol. 76, pp 166–169, March 1972.
- [9] Guest J. The buckling of uniformly compressed parallelogram plates having all edges clamped. Technical Report ARL-SM-172, Aeronautical research laboratories, Australia, 1951.
- [10] Guest J. The compressive buckling of a parallelogram plate simply supported along all four edges. Technical Report ARL-SM-199, Aeronautical Research Laboratories, Australia, 1952.
- [11] Jaunky N, Knight Jnr N, and Ambur D. Buckling of arbitrary quadrilateral anisotropic plates. *AIAA Journal*, Vol. 33, No 5, pp 938–944, May 1995.
- [12] Kennedy J. B and Prabhakara M. K. Buckling of simply supported orthotropic skew plates. *The Aeronautical Quarterly*, Vol. 29, pp 161–172, 1978.
- [13] Mizusawa T and Kajita T. Vibration and buckling of skew plates with edges elastically restrained against rotation. *Computers and Structures*, Vol. 22, No 6, pp 987–994, 1986.
- [14] Mizusawa T, Kajita T, and Naruoka M. Analysis of skew plate problems with various constraints. *Journal of Sound and Vibration*, Vol. 73, No 4, pp 575–584, 1980.
- [15] Mizusawa T, Kajita T, and Naruoka M. Buckling of skew plate structures using B-spline functions. *International Journal for Numerical Methods in Engineering*, Vol. 15, pp 87–96, 1980.
- [16] Mizusawa T and Leonard J. W. Vibration and buckling of plates with mixed boundary conditions. *Engineering Structures*, Vol. 12, pp 285–290, Oct 1990.
- [17] Morley L. S. D. *Skew Plate and Structures*. Pergamon Press, Oxford, 1963.
- [18] Timoshenko S. *Theory of Elastic Stability*. 2 edition, Engineering Science Monograph, McGraw Hill, 1961.
- [19] Wittrick W. H. Buckling of oblique plates with clamped edges under uniform compression. *The Aeronautical Quarterly*, , No 4, pp 151–163, February 1953.
- [20] Wittrick W. H. Buckling of oblique plates with clamped edges under uniform shear. *The Aeronautical Quarterly*, Vol. 5, pp 39–51, May 1954.
- [21] Xiang Y, Wang C. M, and Kitipornchai S. Shear buckling of simply supported skew mindlin plates. *AIAA Journal*, Vol. 33, No 2, pp 377–378, 1994.
- [22] York C. B. Influence of continuity and aspect ratio on buckling of skew plates and plate assemblies. *International Journal of Solids and Structures*, Vol. 33, No 15, pp 2133–2159, 1996.
- [23] York C. B. Buckling design curves for isotropic rectangular plates with continuity or elastic edge restraints against rotation. *Aeronautical Journal*, 2000. In Press.
- [24] York C. B and Williams F. W. Theory and buckling results for infinitely wide stiffened skew plate assemblies. *Composite Structures*, Vol. 28, pp 189–200, 1994.
- [25] Yoshimura Y and Iwata K. Buckling of simply supported oblique plates. *Journal of Applied Mechanics*, Vol. 30, No 2, pp 363–366, September 1963.